XY-Ashkin-Teller Phase Diagram in d=2: Multipilicity of Algebraic Order

E. Can Artun[1,2] and A. Nihat Berker[2,3,4]
[1] *TÜBITAK Research Institute for Fundamental Sciences, Gebze, Kocaeli 41470, Turkey*
[2] *Faculty of Engineering and Natural Sciences, Kadir Has University, Cibali, Istanbul 34083, Turkey*
[3] *TÜBITAK Research Institute for Basic Sciences, Gebze, Kocaeli 41470, Turkey*
[4] *Department of Physics, Massachusetts Institute of Technology, Cambridge, Massachusetts 02139, USA*

A multiplicity of algebraic order is found in the phase diagram of the Ashkin-Tellerized XY model in spatial dimension $d = 2$, in the form of renormalization-group fixed lines and fixed surfaces. In this system, each site has two continuously varying spins, each spin being an XY spin, that is having orientation continuously varying in 2π radians. Nearest-neighbor sites are coupled by two-spin and four-spin interactions. The phase diagram has algebraically ordered phases that are ferromagnetic and antiferromagnetic in each of the spins, and algebraically ordered phases that are ferromagnetic and antiferromagnetic in the combined spin variable. The former two phases are subtended two multiplicative BKT fixed lines. The latter two phases are subtended by fixed surfaces. The evolution of continuously varying criticality is traced within each of the four phases. The renormalization-group flows, the fixed lines and the fixed surfaces are in terms of the doubly composite Fourier coefficients of the exponentiated energy of the four nearest-neighbor spins.

I. CONTINUOUSLY VARIABLE CRITICAL EXPONENTS IN THE XY ASHKIN-TELLER COMPLEXITY

A distinctive low-temperature phase which actually is a continuously varying continuum of critical points, with absence of length scale, is seen in spatial dimension $d = 2$ in the XY model,

$$-\beta\mathcal{H} = \sum_{\langle ij\rangle} J\, \vec{s}_i \cdot \vec{s}_j \qquad (1)$$

where $\beta = 1/k_BT$ is the inverse temperature, at each site i there is an XY unit spin $\vec{s}_i$ that can point in 2π directions, and the sum is over all pairs of spins on nearest-neighbor sites.

On the other hand, the conventional Ashkin-Teller model [1–3] is a doubled-up progeny of the up-down spin Ising model, ushering a multiplicity of order parameters and ordered phases from this discrete-spin model. Using continously orientable XY spins instead of discrete Ising spins, with the algebraic ordering of $d = 2$, brings a multiplicity of algebraic order. The resulting model is defined by the Hamiltonian

$$-\beta\mathcal{H} = \sum_{\langle ij\rangle} [J(\vec{s}_i \cdot \vec{s}_j + \vec{t}_i \cdot \vec{t}_j) + M(\vec{s}_i \cdot \vec{s}_j)(\vec{t}_i \cdot \vec{t}_j)] = \sum_{\langle ij\rangle} -\beta\mathcal{H}_{ij}(\vec{s}_i, \vec{t}_i; \vec{s}_j, \vec{t}_j) \qquad (2)$$

where at each site i there are two XY unit spins $\vec{s}_i, \vec{t}_i$ that can point in 2π directions, and the sum is over all interacting quadruples of spins on nearest-neighbor pairs of sites.

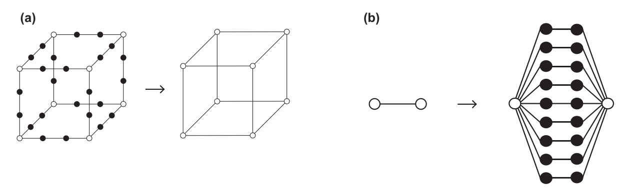

FIG. 1. (a) The Migdal-Kadanoff approximate renormalization-group transformation on the cubic lattice. Bonds are removed from the cubic lattice to make the renormalization-group transformation doable. The removed bonds are compensated by adding their effect to the decimated remaining bonds. (b) A hierarchical model is constructed by self-imbedding a graph into each of its bonds, *ad infinitum*.[6] The exact renormalization-group solution proceeds in the reverse direction, by summing over the internal spins shown with the dark circles. Here is the most used, so called "diamond" hierarchical lattice [6–9]. The length-rescaling factor b is the number of bonds in the shortest path between the external spins shown with the open circles, $b = 3$ in this case. The volume rescaling factor b^d is the number of bonds replaced by a single bond, $b^d = 27$ in this case, so that $d = 3$.

II. METHOD: DOUBLE FOURIER EXPANSION OF TWO CONTINUOUS ANGLES

The renormalization-group transformation, explained in Fig. 1, is done with length rescaling factor $b = 3$ in order to conserve the ferromagnetic-antiferromagnetic symmetry of the method. This method [4, 5] involves decimating three bonds in series into a single bond, followed by bond-moving by superimposing $b^{d-1} = 9$ bonds. This approach is an approximate solution on the $d = 3$ cubic lattice and, simultaneously, an exact solution on the $d = 3$ hierarchical lattice [6–9]. The simultaneous exact solution makes the approximate solution a physically realizable, therefore robust approximation, as also used in turbulence [10], polymer [11], gel [12], electronic system [13] calculations. For recent works on hierarchical lattices, see Refs.[14–27]

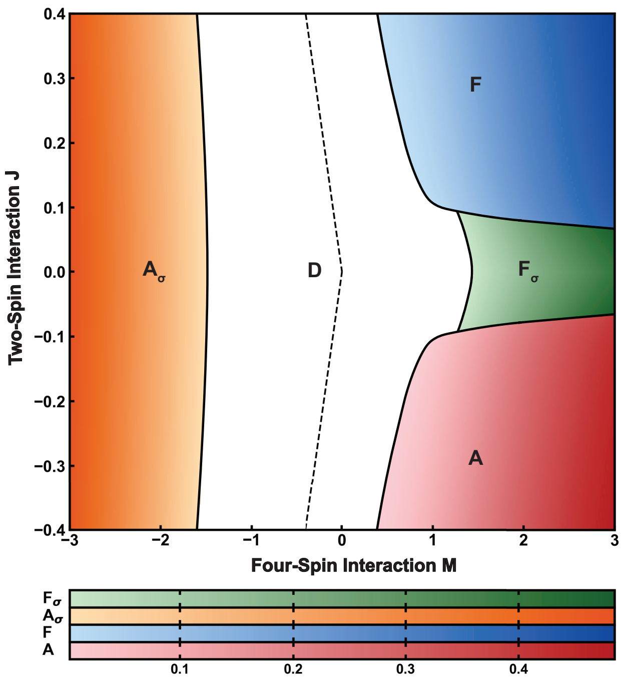

FIG. 2. Calculated phase diagram of the XY Ashkin-Teller model. The ferromagnetic (F) and antiferromagnetic (A) phases of the continuously orientable spin variables $\vec{s}_i$ and $\vec{t}_i$, and the ferromagnetic (F_σ) and antiferromagnetic (A_σ) phases of the composite spin variable $\vec{s}_i\vec{t}_i$, and the disordered phase (D) are shown. The coloring shows the continuously varying criticality of the algebraically ordered phases, the coloring indicating the numerical value of the final destination, on the fixed line or fixed surface, of the renormalization-group trajectory.

As part of the first, decimation, step of the renormalization-group transformation, a decimated bond is obtained by integrating over the shared two spins of two bonds. With $u_{ij}(\theta_{ij},\varphi_{ij}) = e^{-\beta\mathcal{H}_{ij}(\vec{s}_i,\vec{t}_i;\vec{s}_j,\vec{t}_j)}$ being the exponentiated nearest-neighbor Hamiltonian between sites (i,j), and $\theta_{ij}=\theta_i-\theta_j$ and $\varphi_{ij}=\varphi_i-\varphi_j$ being the angles between the planar unit vectors $(\vec{s}_i,\vec{s}_j)$ and $(\vec{t}_i,\vec{t}_j)$, decimation proceeds as

$$\tilde{u}_{13}(\theta_{13},\varphi_{13}) = \int_0^{2\pi} u_{12}(\theta_{12},\varphi_{12})u_{23}(\theta_{23},\varphi_{23})\frac{d\theta_2}{2\pi}\frac{d\varphi_2}{2\pi}. \tag{3}$$

Using the double Fourier transformation [28, 29]

$$f(k,l) = \int_0^{2\pi} u(\theta,\varphi)e^{ik\theta+il\varphi}\frac{d\theta}{2\pi}\frac{d\varphi}{2\pi},$$
$$u(\theta,\varphi) = \sum_{k=-\infty}^{\infty}\sum_{l=-\infty}^{\infty} e^{-ik\theta-il\varphi}f(k,l), \tag{4}$$

the decimation of Eq.(2) becomes

$$\tilde{f}_{13}(k,l) = f_{12}(k,l)f_{23}(k,l). \tag{5}$$

As part of the second, bond-moving, step of the renormalization-group transformation, a bond moving is effected as

$$u'_{ij}(\theta,\varphi) = \tilde{u}_{i_1j_1}(\theta,\varphi)\,\tilde{u}_{i_2j_2}(\theta,\varphi),$$
$$f'_{ij}(k,l) = \sum_{m=-\infty}^{\infty}\sum_{n=-\infty}^{\infty}\tilde{f}_{i_1j_1}(k-m,l-n)\tilde{f}_{i_2j_2}(m,n). \tag{6}$$

We have followed the renormalization-group flows in terms of the $k=0$ to 20 and $l=0$ to 20 double Fourier components, also using $f_{ij}(k,l)=f_{ij}(-k,l)=f_{ij}(k,-l)=f_{ij}(-k,-l)$. We also made spot checks with higher number of double Fourier components (up to $k,l=0$ to 100). We set to unity the maximum value of the double Fourier components, by dividing with the same constant (the raw maximal value), which amounts to adding the same constant to all energies.

III. RESULTS: PHASE DIAGRAM, ENTROPIC ORDERED PHASES, REVERSE BIFURCATION

The phase diagram (Fig. 2) is obtained by following the renormalization-group flows of the double Fourier components, obtained as described above, to their stable fixed points, namely sinks. The basin of attraction of each sink is a corresponding thermodynamic phase.[30] In this XY-Ashkin-Teller model, there are five sinks and therefore five distinct thermodynamic phases. The exponentiated nearest-neighbor interactions, $u_{ij}(\theta_{ij},\varphi_{ij}) = e^{-\beta\mathcal{H}_{ij}(\vec{s}_i,\vec{t}_i;\vec{s}_j,\vec{t}_j)}$, reconstructed [Eq.(3)] from the double Fourier coefficients, at four of these sinks are shown in Fig. 3. A sink epitomizes the ordering of its corresponding thermodynamic phase that it attracts under renormalization group. Thus, as seen leftmost in Fig. 3, in the ferromagnetic phase F, the $\vec{s}_i$ spins are aligned ($\theta_{ij}=0$) with each other and separately the $\vec{t}_i$ spins are aligned ($\varphi_{ij}=0$) with each other. In the antiferromagnetic phase A, the neighboring $\vec{s}_i$ spins are antialigned ($\theta_{ij}=\pi$) with each other and separately the neighboring $\vec{t}_i$ spins are antialigned ($\varphi_{ij}=\pi$) with each other. In the entropic composite ferromagnetic phase F_σ, the neighboring spins $\vec{s}_i=\pm\vec{s}_j$ and simultaneously $\vec{t}_i=\pm\vec{t}_j$, the upper (or lower) signs being jointly valid, $\theta_{ij},\varphi_{ij}=0$ or π. In the also entropic composite antiferromagnetic phase, in neighboring (s_i,s_j) and (t_i,t_j) are either respectively aligned and antialigned, or respectively antialigned and aligned. The latter two ordered phases have an entropy per bond $S/N=\ln 2$. Furthermore, in all four ordered phases, the relative orientation of the s_i and t_i systems has a global degeneracy of 2π. The sink of the disordered phase (not shown in Fig. 3) has

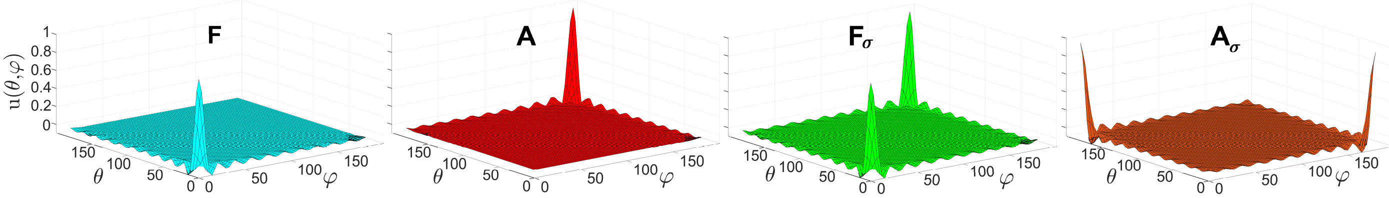

FIG. 3. Renormalization-group sinks of the phases of the XY Ashkin-Teller model. The exponentiated nearest-neighbor energy $u_{ij} = e^{-\beta \mathcal{H}_{ij}(\vec{s}_i,\vec{t}_i;\vec{s}_j,\vec{t}_j)}$ is shown, as a function of the angle θ between the spins $\vec{s}_i, \vec{s}_j$ and the angle φ between the spins $\vec{t}_i, \vec{t}_j$. The energies are normalized to the maximum value of $u = 1$ by the inclusion of an additive constant to the energy.

the (0,0) double Fourier component equal to unity, all other double Fourier components equal to zero. Therefore, $u_{ij}(\theta_{ij}, \varphi_{ij}) = e^{-\beta \mathcal{H}_{ij}(\vec{s}_i,\vec{t}_i;\vec{s}_j,\vec{t}_j)} = 1$ independent of angle. Calculated phase diagram exhibits (inset of Fig. 2) a reverse bifurcation where a phase boundary splits into two phase boundaries and one of the latter reverses direction. This phenomenon occurs symmetrically at positive and negative J.

IV. CONCLUSION

We have solved, by renormalization-group theory, the Ashkin-Teller type doubled-up XY magnetic spin model in spatial dimension $d = 3$. We find four different ordered phases, with ferromagnetic and antiferromagnetic orderings of the direct and composite spins. Two reverse bifurcations, where a phase boundary splits into two phase boundaries and one of the latter reverses directions, occurs symmetrically at positive and negative J.

ACKNOWLEDGMENTS

Support by the Academy of Sciences of Turkey (TÜBA) is gratefully acknowledged.

[1] J. Ashkin and E. Teller, Statistics of Two-Dimensional Lattices with Four Components, Phys. Rev. **64**, 178 (1943).

[2] R. V. Ditzian, J. R. Banavar, G. S. Grest, and L. P. Kadanoff, Phase Diagram for the Ashkin-Teller Model in Three Dimensions, Phys. Rev. B **22**, 2542 (1980).

[3] I. Keçoğlu and A. N. Berker, Global Ashkin–Teller Phase Diagrams in Two and Three dimensions: Multicritical Bifurcation versus Double Tricriticality-Endpoint, Physica A **30**, 129248 (2023).

[4] A. A. Migdal, Phase transitions in gauge and spin lattice systems, Zh. Eksp. Teor. Fiz. **69**, 1457 (1975) [Sov. Phys. JETP **42**, 743 (1976)].

[5] L. P. Kadanoff, Notes on Migdal's recursion formulas, Ann. Phys. (N.Y.) **100**, 359 (1976).

[6] A. N. Berker and S. Ostlund, Renormalisation-group calculations of finite systems: Order parameter and specific heat for epitaxial ordering, J. Phys. C **12**, 4961 (1979).

[7] R. B. Griffiths and M. Kaufman, Spin systems on hierarchical lattices: Introduction and thermodynamic limit, Phys. Rev. B **26**, 5022R (1982).

[8] M. Kaufman and R. B. Griffiths, Spin systems on hierarchical lattices: 2. Some examples of soluble models, Phys. Rev. B **30**, 244 (1984).

[9] A. N. Berker and S. R. McKay, Hierarchical Models and Chaotic Spin Glasses, J. Stat. Phys. **36**, 787 (1984).

[10] R. H. Kraichnan, Dynamics of Nonlinear Stochastic Systems, J. Math. Phys. **2**, 124 (1961).

[11] P. J. Flory, Principles of Polymer Chemistry (Cornell University Press: Ithaca, NY, USA, 1986).

[12] M. Kaufman, Entropy Driven Phase Transition in Polymer Gels: Mean Field Theory, Entropy **20**, 501 (2018).

[13] P. Lloyd and J. Oglesby, Analytic Approximations for Disordered Systems, J. Phys. C: Solid St. Phys. **9**, 4383 (1976).

[14] E. C. Artun, D. Sarman, and A. N. Berker, Nematic Phase of the n-Component Cubic-Spin Spin Glass in d=3: Liquid-Crystal Phase in a Dirty Magnet, Physica A **40**, 129709 (2024).

[15] Y. E. Pektaş, E. C. Artun, and A. N. Berker, Driven and Non-Driven Surface Chaos in Spin-Glass Sponges, Chaos, Solitons and Fractals **17**, 114159 (2023).

[16] J. Clark and C. Lochridge, Weak-disorder limit for directed polymers on critical hierarchical graphs with vertex disorder, Stochastic Processes Applications **158**, 75 (2023).

[17] M. Kotorowicz and Y. Kozitsky, Phase transitions in the Ising model on a hierarchical random graph based on the triangle, J. Phys. A **55**,405002 (2022).

[18] P. P. Zhang, Z. Y. Gao, Y. L. Xu, C. Y. Wang, and X. M. Kong, Phase diagrams, quantum correlations and critical phenomena of antiferromagnetic Heisenberg model on diamond-type hierarchical lattices, Quantum Science

Technology **7**, 025024 (2022).

[19] K. Jiang, J. Qiao, and Y. Lan, Chaotic Renormalization Flow in the Potts model induced by long-range competition, Phys. Rev. E **103**, 062117 (2021).

[20] G. Mograby, M. Derevyagin, G. V. Dunne, and A. Teplyaev, Spectra of perfect state transfer Hamiltonians on fractal-like graphs, J. Phys. A **54**, 125301 (2021).

[21] I. Chio, R. K. W. Roeder, Chromatic zeros on hierarchical lattices and equidistribution on parameter space, Annales de l'Institut Henri Poincaré D, **8**, 491 (2021).

[22] B. Steinhurst and A. Teplyaev, Spectral analysis on Barlow and Evans' projective limit fractals, J. Spectr. Theory **11**, 91 (2021).

[23] A. V. Myshlyavtsev, M. D. Myshlyavtseva, and S. S. Akimenko, Classical lattice models with single-node interactions on hierarchical lattices: The two-layer Ising model, Physica A **558**, 124919 (2020).

[24] M. Derevyagin, G. V. Dunne, G. Mograby, and A. Teplyaev, Perfect quantum state transfer on diamond fractal graphs, Quantum Information Processing, **19**, 328 (2020).

[25] S.-C. Chang, R. K. W. Roeder, and R. Shrock, q-Plane zeros of the Potts partition function on diamond hierarchical graphs, J. Math. Phys. **61**, 073301 (2020).

[26] C. Monthus, Real-space renormalization for disordered systems at the level of large deviations, J. Stat. Mech. - Theory and Experiment, 013301 (2020).

[27] O. S. Sarıyer, Two-dimensional quantum-spin-1/2 XXZ magnet in zero magnetic field: Global thermodynamics from renormalisation group theory, Philos. Mag. **99**, 1787 (2019).

[28] J. V. José, L. P. Kadanoff, S. Kirkpatrick, and D. R. Nelson, Renormalization, vortices, and symmetry-breaking perturbations in two-dimensional planar model, Phys. Rev. B **16**, 1217 (1977).

[29] A. N. Berker and D. R. Nelson, Superfluidity and Phase Separation in Helium Films, Phys. Rev. B **19**, 2488 (1979).

[30] A. N. Berker and M. Wortis, Blume-Emery-Griffiths-Potts Model in Two Dimensions: Phase Diagram and Critical Properties from a Position-Space Renormalization Group, Phys. Rev. B **14**, 4946 (1976).